

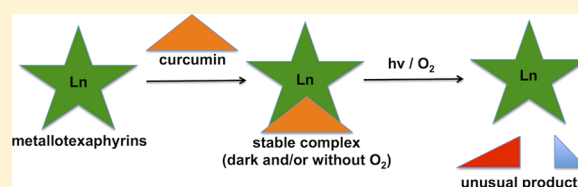
Lanthanide Texaphyrins as Photocatalysts

Aaron D. Lammer, Grégory Thiabaud,¹ James T. Brewster II,¹ Julie Alaniz, Jon A. Bender,¹ and Jonathan L. Sessler^{*1}

Department of Chemistry, The University of Texas at Austin, 105 East 24th Street, Stop A5300, Austin, Texas 78712-1224, United States

Supporting Information

ABSTRACT: Here, we report the use of gadolinium(III)-, lutetium(III)-, and lanthanum(III)-texaphyrins as bioinspired photocatalysts that promote a novel approach to the degradation of curcumin, a 1,3-diketo-containing natural product. Complexation of curcumin to the lanthanide centers of the texaphyrins yields stable species that display limited reactivity in the dark or under anaerobic conditions. However, upon exposure to mWatt intensity light (pocket flashlight) or simply under standard laboratory illumination in the presence of atmospheric oxygen, substrate oxidation occurs readily to generate curcumin-derived cleavage products. These latter species were identified on the basis of spectroscopic and mass spectrometric analyses. The mild nature of the activation conditions serves to highlight a potential new role for photoactive lanthanide complexes.



INTRODUCTION

Catalysis is a mainstay of modern organic synthesis, and many groups continue to search for new catalysts. Much of this search has focused on late transition metals such as iridium, ruthenium, and platinum. However, many of these metals are rare and expensive. By comparison, lanthanide metals are relatively abundant. However, they have not been as thoroughly studied as catalysts.^{1–4} To date, lanthanide complexes have mainly been exploited as Lewis acids in aldol- and Michael-type reactions.¹ They have also been studied extensively in the context of nucleic acid ester hydrolysis.^{5,6} In very recent work by the Schelter group, a synthetic model of a Ln-dependent dehydrogenase enzyme was put forth.⁷ However, there are still relatively few studies that exploit lanthanide complexes as photocatalysts.^{8–11} Recently, the Patra group utilized Eu(III) and Tb(III) β -diketonate complexes to effect DNA cleavage under conditions of intense UV photoirradiation (365 nm, 6 W).¹² Here, we report that the gadolinium(III)-, lutetium(III)-, and lanthanum(III) texaphyrins (MGd, MLu, and MLa, respectively; Scheme 1) form stable complexes with curcumin in the absence of oxygen or light. Upon exposure to O₂ and a relatively low energy light source (e.g., a pocket flashlight or sunlight filtered through a window), curcumin undergoes cleavage in the presence of these trivalent lanthanide texaphyrin complexes. The catalytic transformations induced in this way represent the formal converse of the biosynthesis of curcumin from feruloyl-diketide-COA mediated by curcumin synthase (CURS).

Texaphyrins are pentadentate expanded porphyrins that can form highly stable complexes with trivalent lanthanide ions. They have been studied extensively with regard to their chemical and photophysical properties.^{13–15} For example, lutetium texaphyrins (e.g., MLu) have been utilized as photosensitizers for photodynamic therapy (PDT) and are

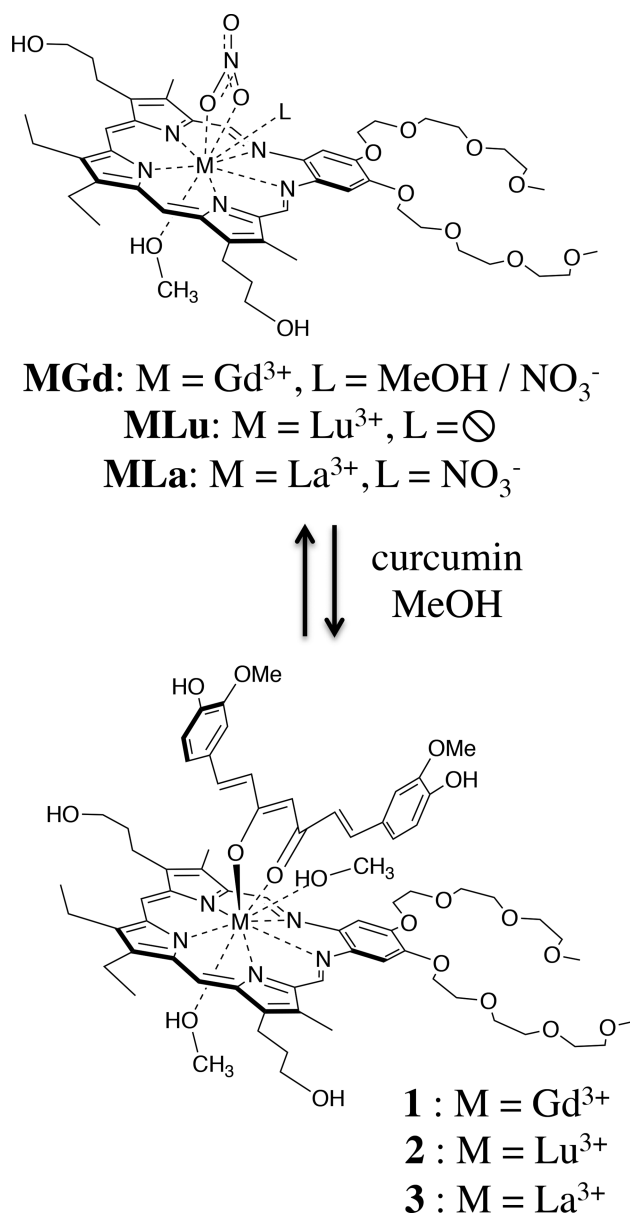
known to generate reactive oxygen species (ROS) under appropriately chosen conditions.^{16,17} Dysprosium(III) texaphyrin complexes have been used as ribozyme analogues capable of effecting site-directed cleavage of RNA.¹⁸ Additionally, gadolinium texaphyrins (e.g., MGd) can function as redox mediators.^{19,20}

In the solid state, lanthanide(III)-texaphyrins are characterized by the presence of neutral and anionic axial ligands.²¹ This led us to consider that lanthanide(III)-texaphyrin complexes might interact with multidentate ligands containing a 1,3-diketone functionality. One such diketone, curcumin, has been studied for a range of conditions from cancer to Alzheimer's disease.^{22–26} However, there is still debate over the actual salutary roles, if any, curcumin or its metabolites play in a physiological setting.²⁷

Curcumin is a natural product isolated from turmeric. It has long been sought for its purported medicinal properties, including as an antioxidant, as well as for many other purposes.^{28,29} Curcumin is readily broken down to vanillin and similar molecules in organic solvents.²⁸ These products are also seen under physiological conditions, in addition to bicyclic species resulting from autoxidation and cyclization as reported by Schneider.³⁰ This reactivity has been mediated by ligation to numerous metals.³¹ However, these unique chemistries, coupled with the recognized importance of the β -diketo moiety in certain pharmaceutical agents,³² led us to explore whether chelation of curcumin to lanthanide texaphyrins could be used to create species with greater stability to solvolysis and whether, once prepared, these latter putative complexes could be degraded under relatively mild conditions in a controlled fashion. In purely chemical terms, the challenge we sought to

Received: January 29, 2018

Scheme 1. Proposed Structures of the Complexes of Curcumin and Metallotexaphyrins MGd, MLu, and MLa²¹ Based on Evidence Obtained from Mass Spectrometric, UV–Vis Spectroscopic, ITC, and in the case of MLu and MLa, ¹H NMR Spectroscopic Analyses



address is whether it would be possible to use lanthanide texaphyrin chemistry both to stabilize and decompose catalytically an inherently unstable natural product. As detailed below, we were able to achieve both goals.

RESULTS AND DISCUSSION

Characterization of Metallotexaphyrin–Curcumin Complexes. Evidence for the formation of MGd, MLu, and MLa curcumin complexes came from UV–vis spectroscopy, isothermal calorimetry (ITC), mass spectrometry, and in the case of the diamagnetic MLu and MLa complexes, ¹H NMR spectroscopy. Data acquired from these studies proved consistent with a 1:1 binding stoichiometry following initial texaphyrin axial ligand dissociation. ITC analyses revealed an endothermic coordination event for all 3 complexes³³ and

apparent affinity constants that range from 7.2×10^3 to 2.8×10^5 M⁻¹. The affinities increase with the size of the lanthanide cation (La(III) > Gd(III) > Lu(III)), a finding explained by the fact that the larger cations reside further from the plane formed by the texaphyrin ligand, making the metal center more accessible to the curcumin substrate.²¹ The complexation to MLa or MGd is entropically favored because it releases two axial ligands vs only one for MLu (Scheme 1).

Upon addition of excess curcumin to solutions of MGd, MLu, or MLa in methanol, the intense Soret band seen in the UV–vis spectrum that is characteristic of these metallotexaphyrins decreases. Furthermore, a 5–7 nm bathochromic shift in the Q-band is seen (Figure 1). These results lead us to suggest that curcumin interacts with these metallotexaphyrins via an axial coordination mode as proposed in Scheme 1.

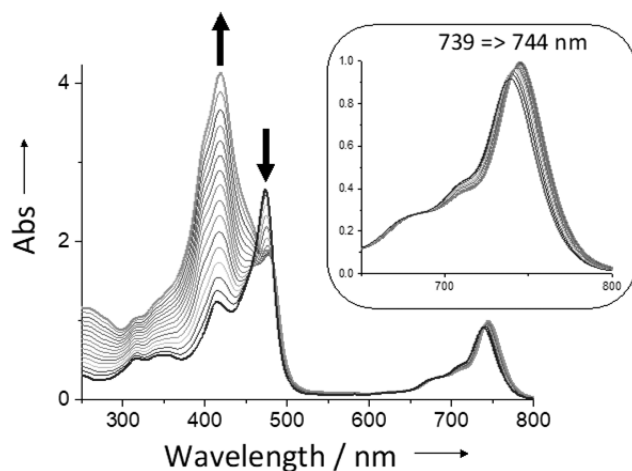


Figure 1. UV–vis (MeOH, 300 K, dark) spectra of MGd (30 μM) + curcumin (added in 0.1 equiv increments; total added = 1.5 equiv). Note: The higher energy band is due to curcumin, whereas that at ca. 480 nm is ascribed to MGd (free and complexed).

A ¹H NMR spectroscopic titration of curcumin into an acetonitrile solution of MLu revealed a shift of the curcumin proton signals to higher field; presumably, this reflects the effect of the texaphyrin ring current. In addition, the *meso*-protons of MLu undergo a shift from 9.08 and 11.91 ppm to 9.71 and 12.15 ppm, respectively (see Supporting Information Figure S19). These results lead us to suggest that modifications to the electronic structure of the texaphyrin core take place as the result of the presumed curcumin complexation.

Stability studies. The stability of complex 1 was initially probed using UV–vis spectroscopy for samples made up in a 1:1 mixture of MeOH/PBS in the dark at 37 °C. Corresponding control studies involving curcumin alone were also carried out. The decrease in the band at 420 nm (ascribed to curcumin) is much slower when curcumin is bound to MGd: Half of the curcumin (alone) is degraded after 5.5 h, whereas 70% of curcumin bound to MGd is still present after 16 h (cf. Figure S25). On this basis we conclude that the rate of decomposition of curcumin is reduced upon complex formation (cf. Supporting Information).³⁴ MGd is appreciably soluble in aqueous media. Thus, the same stability experiment could be carried out in an aqueous solution containing only 0.6% methanol. Again, 1 was observed to be more stable than curcumin alone under those conditions as inferred from monitoring analogous time dependent optical spectral changes.

In this particular case, complexation to MGd slows curcumin hydrolysis and prevents precipitation.

In the dark or in the absence of O₂, millimolar methanolic solutions of complexes **1** and **2** were stable for several days on the benchtop. However, in the presence of 5 equiv of curcumin, complex **3** degraded in several hours at room temperature. The color of the solution goes from green to red, and HPLC/UV-vis analysis revealed the degradation of the La(III) texaphyrin core. This lack of stability for the curcumin complex of MLa led us to focus mainly on MGd and MLu for the present study. In this context, we were particularly keen to see if these two lanthanide(III) complexes would function as catalysts for curcumin photodegradation.

Upon exposure first to O₂, either via bubbling or through contact with the laboratory atmosphere, followed by subjecting complexes **1** or **2** to photoillumination with a flashlight or exposure to ambient laboratory light, the spectral changes shown in Figure 2 were observed. On the basis of accompanying LC-MS studies, these spectral changes were ascribed to modifications in the curcumin core structure.

Photoreactivity Studies. Upon irradiation with a 225 mW pocket flashlight, the Soret band increases, whereas the intensity of the absorption feature at 420 nm, ascribed to curcumin, decreases. The maximum of the Q-band shifts back to 739 nm and matches the initial wavelength of this metallotexaphyrin (i.e., MGd). These observations lead us to suggest that the resultant metabolites dissociate from the metal center. Further analysis of the reaction mixture by RP-HPLC and LC-MS provided support for the suggestion that curcumin is converted into two major products with complete retention of the texaphyrin structure. Indeed, no apparent change in the texaphyrin spectral features were observed. We thus conclude that the photochemistry is catalytic in texaphyrin with the induced chemical changes occurring solely within the curcumin skeleton.

The two main daughter products produced as the result of photoirradiation display close retention times on the RP-HPLC C18 column (Figure 2C, peaks B and C, 9.7 vs 9.9 min). Peak B absorbs at both 254 and 420 nm while C absorbs only at 254 nm. Based upon these observations, we infer that product B likely displays conjugation between the aromatic rings and unsaturated open chains in analogy to what is seen in curcumin. Product B is thus considered to be a larger (i.e., higher molecular weight) breakdown fragment than peak C. LC-MS analyses support these conclusions in that presumed molecular ion peaks at 236 and 154 amu are seen for B and C, respectively.

An intermediate peak A is also observed in the RP-HPLC chromatogram. An LC-MS analysis of peak A revealed a mass of 439 g/mol (sodium adduct).

The effect of the curcumin/metallotexaphyrin ratio on the reaction was tested. It was found that the conversion of curcumin to products B and C was complete in the presence of air and light, even when curcumin was used in excess (e.g., 100 equiv). This finding provides further support for the conclusion that the metallotexaphyrins MGd and MLu can act as photocatalysts for the breakdown of curcumin, rather than serving just as stoichiometric reactants.

The kinetics of the reactions with MLu or MGd as the catalysts were investigated by monitoring the disappearance of curcumin via RP-HPLC. It was observed that the reaction is considerably faster with MGd ($t_{1/2} = 3.1$ min) than with MLu ($t_{1/2} = 12.4$ min) (Figure S29). We hypothesize that this

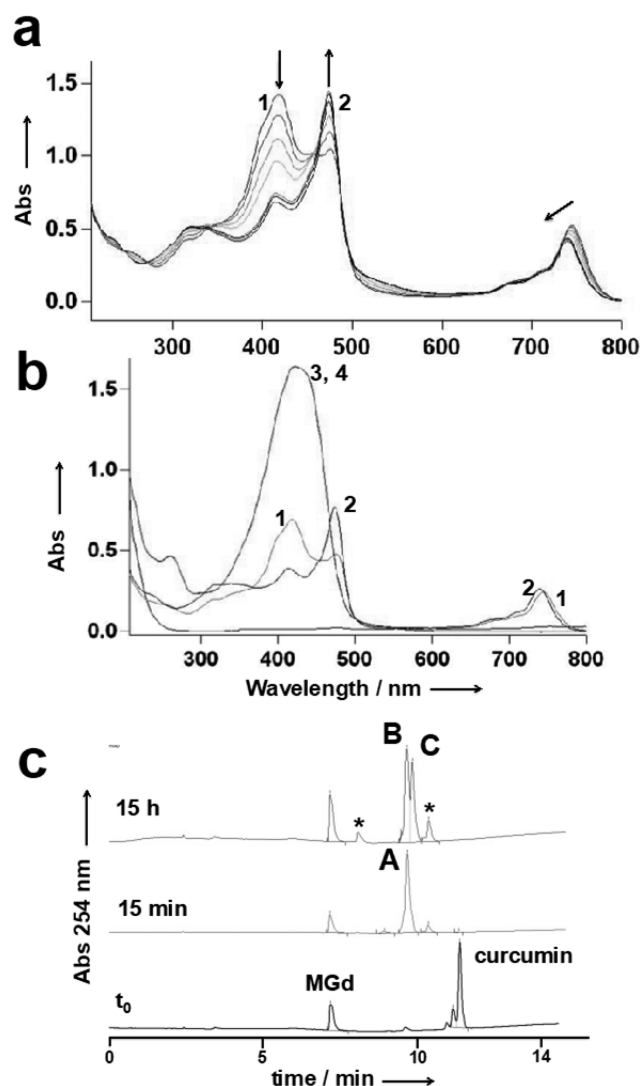


Figure 2. UV-vis spectroscopic analysis of complex **1** (MeOH, rt, $h\nu$). The solution was irradiated with a 225 mW pocket flashlight (a) and monitored by UV-vis spectroscopy over the course of 30 min. Subjecting curcumin alone (b) to similar conditions resulted in no change (i.e., curves 3 and 4). Panel c shows RP-HPLC chromatograms (detector set at 254 nm) of complex **1** before (bottom) and after irradiation for 15 min (middle) with a 225 mW pocket flashlight. The solution was then left in the dark for 15 h (top). Peaks A–C are peaks ascribed to the primary products produced as the result of the proposed photocatalysis. Their identity is discussed in the text proper. * minor byproducts.

difference in rate is related to the difference in binding affinity inferred from the ITC measurements discussed above.

To probe the putative redox chemistry that might underlie the catalytic activity of MGd, electron paramagnetic resonance (EPR) spectroscopic studies were carried out at 90 K in frozen methanol. Analyses were made under anaerobic and aerobic conditions both with and without irradiation (Figure 3). Curcumin itself gives no EPR signal, whereas the Gd(III) center within MGd gives rise to signals at several g -values, namely $g_1 = 5.68$, $g_2 = 2.67$, $g_3 = 2.34$, and $g_4 = 1.98$. Upon addition of curcumin under anaerobic conditions, new signals ascribed to the formation of the MGd–curcumin complex could be observed. Most notably, the intensity of the g_1 signal increases in intensity, while two new peaks, at $g_a = 4.120$ and g_b

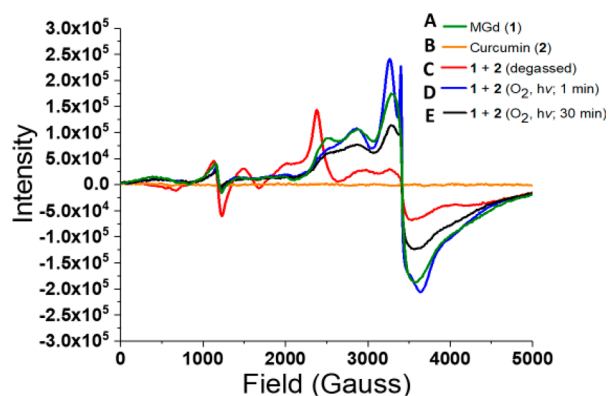


Figure 3. X-band EPR spectra (9.5 GHz) at 90 K of MGd (A), curcumin (B), the presumed MGd–curcumin complex under anaerobic conditions (C), putative MGd–curcumin complex (O_2 , $h\nu$, after 1 min) (D), and MGd–curcumin (O_2 , $h\nu$, after 30 min) (E). All spectra were recorded in methanol. Experimental settings were as follows: amplitude modulation = 10 G and microwave power = 2 mW. The plotted spectra are the average of four scans.

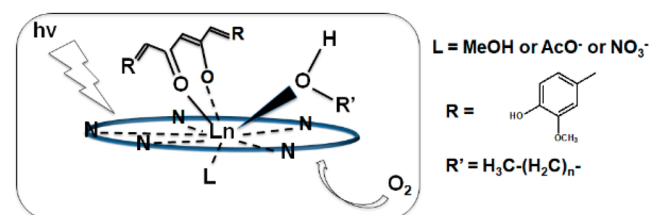
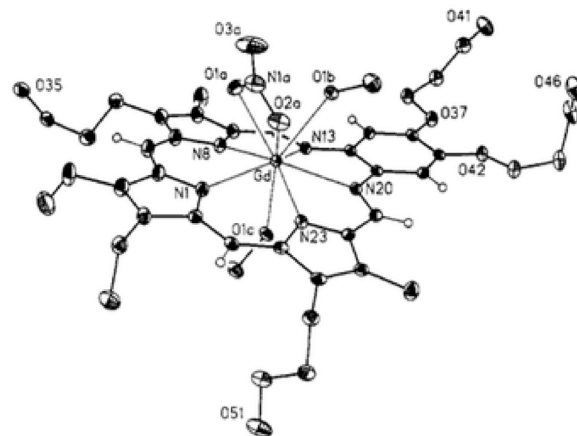
= 2.83, were observed to grow in. A 0.06 shift in the g_3 signal was seen, while the g_4 feature decreased in intensity.

Bubbling the above solution with O_2 and subjecting it to irradiation with low intensity (550 nm 225 mW) light for 1 min led to a slight decrease in the g_1 signal. In addition, the two peaks seen upon initial curcumin complexation, namely at g_a and g_b , were no longer discernible. Conversely, the g_3 and g_4 features were seen to return, albeit at lower intensity than found in MGd. A sharp peak adjacent to g_4 was also observed. This is attributed to the formation of an organic radical localized either on the texaphyrin ring or on an oxidized curcumin derivative. Another set of scans at $t = 30$ min displayed similar g -values with the intensity of the $g_1 = 5.68$ signal being intermediate between that for the MGd–curcumin complex and free MGd. Other less-easily assigned signals were also seen (cf. Figure 3).

Zn(II) tetrapyrrolic porphyrin, protoporphyrin XI, and $\text{Gd}(\text{OAc})_3$ were added to methanolic solutions of curcumin and subsequently oxygenated. Under these conditions no reaction was observed. Nor, were well-known photocatalysts, such as tris(bipyridine)ruthenium(II) or eosin Y, able to promote discernible reactions involving curcumin under conditions of illumination analogous to those used in the case of MGd and MLu. On this basis, we conclude that the macrocyclic ring, as well as the availability of open coordination sites present in these two test lanthanide(III) texaphyrin complexes play critical roles; they may be able to accommodate a molecule of curcumin as well as a molecule of solvent, both of which presumably contribute to the selective degradation of curcumin as shown in Scheme 2.

Curcumin was oxidized in the presence of MGd upon exposure to diffuse laser light whose wavelengths varied from 550 to 800 nm and which ranged in intensity from 1 to 23 mW. The reaction proceeds more slowly in the presence of presumed competitors (i.e., dimethylmalonate or zinc acetate for the MGd and curcumin, respectively). The reaction also slows upon heating. For instance, only 50% degradation of curcumin was seen in the presence of MGd upon exposure to 550 nm 225 mW light at 50 °C for 30 min vs essentially complete reaction at room temperature. From these studies, carried out under otherwise identical conditions, it is concluded

Scheme 2. (Top) Single Crystal X-ray Diffraction Structure Showing the Co-ordination of a Bidentate Ligand (NO_3^-) and a Methanol Molecule to the Same Face of a $\text{Gd}(\text{III})$ Texaphyrin Complex^a and (Bottom) Proposed Active Site Complexation That Presages the Photocatalytic Transformation of a 1,3-Diketo Species Bound to MGd or MLu

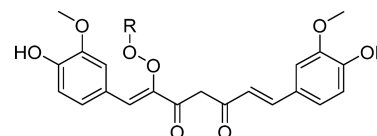


^aReprinted with permission from Sessler et al.²¹ Copyright 1993 American Chemical Society.

that curcumin binding, reduced at higher temperatures, is a prerequisite to photoinduced curcumin degradation.

The proposed photocatalytic degradation reaction was also studied in various alcoholic solvents other than methanol. Monitoring of the presumed intermediate A by LC-MS revealed a correlation between the nature of the alcoholic solvent and the structure of intermediate A (shown in Scheme 3). Importantly, no difference was seen in the mass of the final products B and C (structures in Scheme 4 and discussed below).

Scheme 3. Proposed Structure of Key Intermediate A^a



^aThe R fragment is alcohol derived and varies with the choice of solvent.

Because oxygen appeared necessary for the completion of the photocatalytic reaction, curcumin degradation experiments were carried out in the presence of $^{18}\text{O}_2$ (Figure 4). Under a 50% ^{18}O atom-labeled atmosphere, approximately 50% of the final product B detected in the ESI-MS was characterized by a peak 2 amu (m/z) higher than observed under pure $^{16}\text{O}_2$ (peak

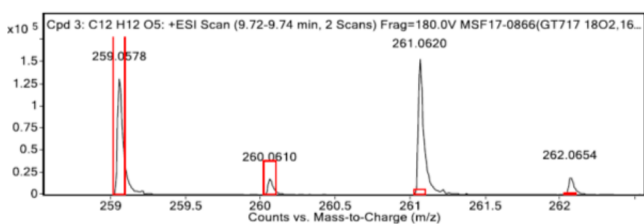
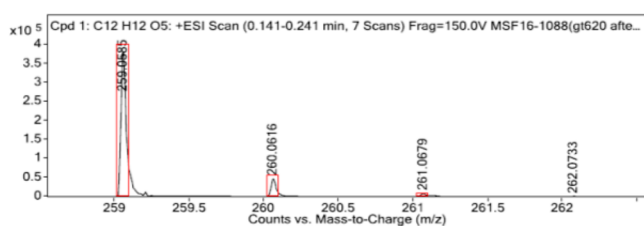
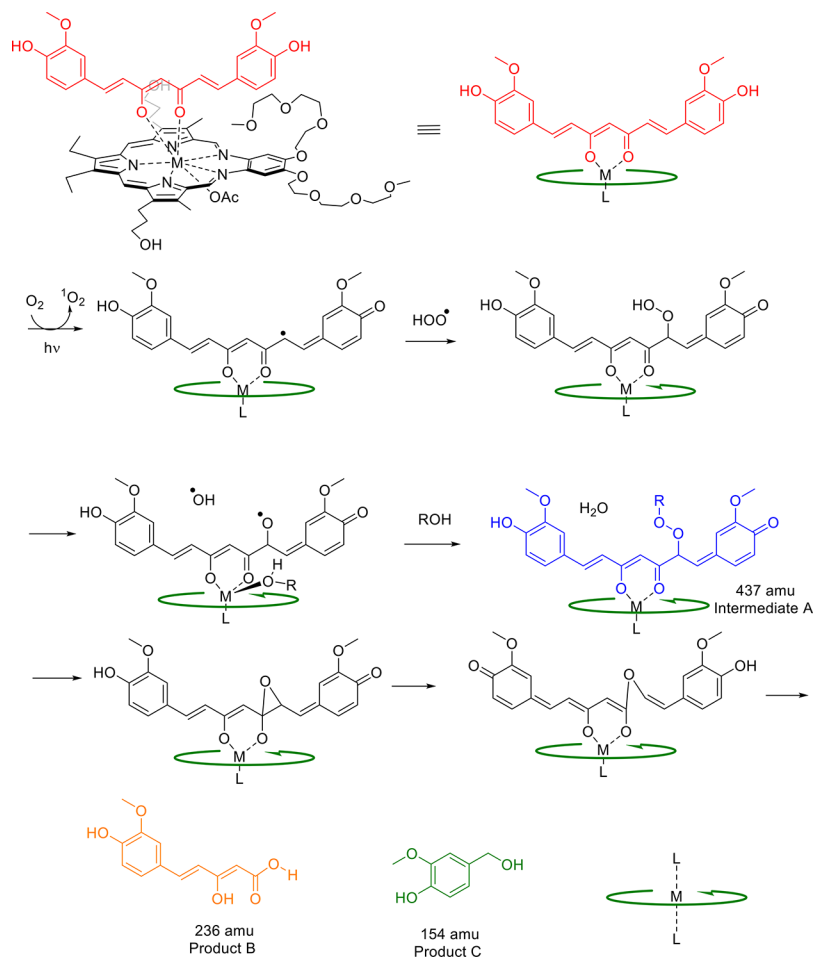
Scheme 4. Proposed Mechanism of Curcumin Photoinduced Oxidation^a

Figure 4. Top: High resolution mass spectrum of compound **B** with ¹⁶O₂. Bottom: High resolution mass spectrum of compound **B** run in the presence of 50% labeled ¹⁸O₂. Both traces correspond to the [M + Na]⁺ adducts.

at amu = 261 vs 259 corresponding to the sodium adducts of the parent peaks at 238 vs 236 *m/z*, respectively). Such findings are consistent with one of the oxygen atoms in **B** coming from the atmosphere (Figure 4, lower portion). The same mass

increment difference was observed for **A** (peak observed at *m/z* = 441 vs 439 for the sodium adducts of the parent peaks at 418 and 416). However, the mass observed for **C** remained unchanged (*m/z* = 177, corresponding to the sodium adduct of the parent peak at 154 amu). On this basis, we conclude that no atmospheric oxygen is inserted into this latter fragment.

IR spectral analysis of the degradation products revealed a carbonyl stretch at 1656 cm⁻¹ in the case of nonlabeled **B**. This feature is broadened and shifted to 1633 cm⁻¹ when the photodegradation reaction is carried out in the presence of ¹⁸O. This latter 1633 cm⁻¹ value corresponds to the average stretch calculated for the ¹⁸O-labeled and ¹⁶O-unlabeled CO-containing products and is thus fully consistent with the observed 50% incorporation of the isotopic label.

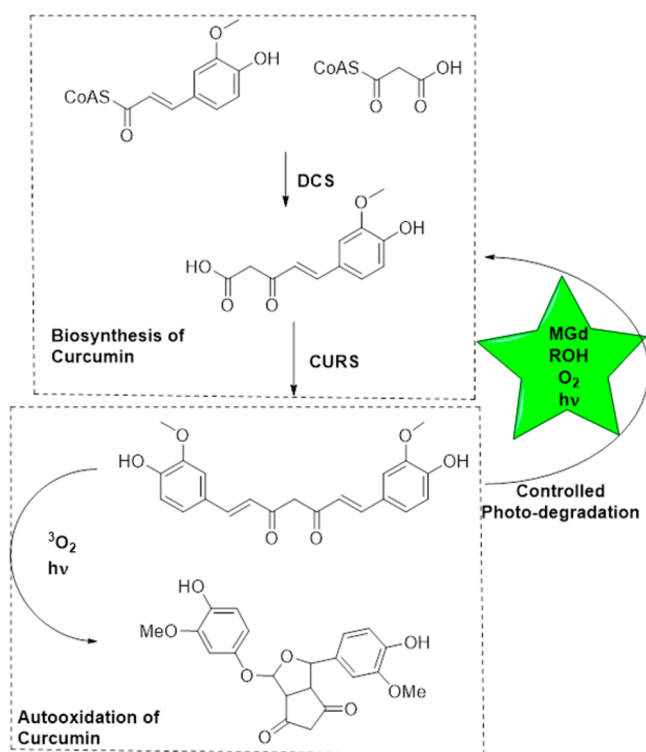
Products **B** and **C** were separated from the metallotexaphyrin catalysts by RP-HPLC and analyzed by 2D-NMR spectroscopic methods (e.g., COSY, TOCSY, HSQC, and HSBC; cf. Supporting Information). The presence of trisubstituted phenyl rings was inferred from the ¹H NMR and COSY spectral experiments. The TOCSY, HSQC, and HSBC spectra provide support for the existence of an ethylene bridge between a phenyl ring and a carbonyl-bearing carbon atom with a CH group being present adjacent to the carbonyl. Taken in concert, these data and the mass spectrometric findings allowed the structure of products **B** and **C** to be assigned; they are shown in Scheme 4.

On the basis of the products produced and inferred intermediates discussed, we propose that curcumin coordinates to the metal center of the lanthanide texaphyrin. This complexation prevents the free radical cyclization involving the two α -positions of curcumin reported by Schneider and coworkers. Instead, the free radical generated on curcumin reacts with singlet oxygen. The coordination of a molecule of solvent to the Gd(III) center close to the bound curcumin favors the formation of intermediate **A**. Protonation and homolytic cleavage of this peroxide species results in formation of the curcumin epoxide. Collapse of the resulting ester enolate and subsequent rearrangement leads to products **B** and **C** and release of the intact metallotexaphyrin. This proposed mechanism is shown in [Scheme 4](#).

CONCLUSION

The results presented here demonstrate that, in the presence of an appropriately chosen lanthanide(III) texaphyrin, it is

Scheme 5. A comparison of the accepted biosynthesis of curcumin (top) compared to the metallotexaphyrin-promoted free radical oxidation reported in the present study (right).³⁶ Also shown is the previously reported free radical oxidation of curcumin (bottom).³⁰



possible to achieve the photoactivated oxidation of curcumin through a novel pathway that can be viewed as being the formal converse of the biosynthesis from feruloyl-diketide-CoA mediated by CURS. This transformation, which is favored in the presence of alcohols, is dependent on the presence of light and oxygen as well as the ability of the 1,3-diketone curcumin substrate to coordinate to the lanthanide(III) texaphyrin core. In aqueous media, the complex is more stable than the substrate alone. This serves to retard formation of the complicated mixture of degradation products usually seen for solutions of curcumin in aqueous media.²⁸ Likely, chelation to

texaphyrin prevents the formation of the bicyclic species previously reported by Schneider and co-workers ([Scheme 5](#)), thus imparting stability.³⁵ Photodegradation is seen in the presence of primary alcohols. Therefore, depending on the conditions, seemingly contrasting behavior is seen in aqueous and alcoholic media in the presence of two representative lanthanide(III) texaphyrins. One set of conditions (aqueous) favors stabilization of curcumin, and the other (alcoholic media) serves to enhance its propensity to undergo light and oxygen-promoted degradation.

The degradation seen in the presence of light and oxygen in the presence of alcoholic solvents is rationalized in terms of the ability of the test lanthanide texaphyrins to coordinate both a diketone substrate and a solvent molecule (*viz.* the alcohol in question) as well as their propensity to produce singlet oxygen and undergo redox changes. Taken in concert, these factors serve to lower the energy barrier for the formation of curcumin radicals. This, in turn, allows for a more controlled radical chemistry. It also permits the use of very low energy light to drive what is overall a very mild photocatalytic process using potentially green sources of energy (*e.g.*, sunlight) and a classically benign oxidizing agent (O_2).

ASSOCIATED CONTENT

Supporting Information

The Supporting Information is available free of charge on the ACS Publications website at DOI: 10.1021/acs.inorgchem.8b00248.

NMR spectra, HRMS data, HPLC spectra, IR spectra, and plots of kinetic data (PDF)

AUTHOR INFORMATION

Corresponding Author

*Phone: 512-471-5009; E-mail: sessler@cm.utexas.edu.

ORCID

Grégory Thiabaud: 0000-0001-5189-8445

James T. Brewster II: 0000-0002-4579-8074

Jon A. Bender: 0000-0003-1713-1480

Jonathan L. Sessler: 0000-0002-9576-1325

Author Contributions

The manuscript was written through contributions of all authors. All authors have given approval to the final version of the manuscript. A.G.L. and G.T. contributed equally.

Funding

This work was supported by the Cancer Prevention and Research Institute of Texas (Grant DP150087 to J.L.S.).

Notes

The authors declare no competing financial interest.

ACKNOWLEDGMENTS

We offer special thanks to Prof. Sean Roberts for use of his laser equipment.

REFERENCES

- (1) Shibasaki, M.; Yoshikawa, N. Lanthanide Complexes in Multifunctional Asymmetric Catalysis. *Chem. Rev.* **2002**, *102*, 2187–2209.
- (2) Li, H.; Zhu, Y.; Cheng, M.; Ren, Z.; Lang, J.; Shen, Q. Lanthanide Chalcogenolate Complexes: Syntheses. *Coord. Chem. Rev.* **2006**, *250*, 2059–2092.

- (3) Edelman, F. T.; Edelman, F. T. Lanthanide Amidinates and Guanidinates in Catalysis and Materials Science: A Continuing Success Story. *Chem. Soc. Rev.* **2012**, *41* (23), 7657.
- (4) Pellissier, H. Recent Developments in Enantioselective Lanthanide-Catalyzed Transformations. *Coord. Chem. Rev.* **2017**, *336*, 96–151.
- (5) Franklin, S. J. Lanthanide-Mediated DNA Hydrolysis. *Curr. Opin. Chem. Biol.* **2001**, *5*, 201–208.
- (6) Desimoni, G.; Faita, G.; Quadrelli, P. Enantioselective Catalytic Reactions with N - Acylidene Penta-Atomic Aza-Heterocycles. Heterocycles as Masked Bricks To Build Chiral Scaffolds. *Chem. Rev.* **2015**, *115*, 9922–9980.
- (7) McSkimming, A.; Cheisson, T.; Carroll, P. J.; Schelter, E. J. Functional Synthetic Model for the Lanthanide-Dependent Quinoid Alcohol Dehydrogenase Active Site. *J. Am. Chem. Soc.* **2018**, *140*, 1223.
- (8) Jenks, T. C.; Bailey, M. D.; Hovey, J. L.; Fernando, S.; Basnayake, G.; Cross, M. E.; Li, W.; Allen, M. J. First Use of a Divalent Lanthanide for Visible-Light-Promoted Photoredox Catalysis. *Chem. Sci.* **2018**, *9*, 1273–1278.
- (9) Yin, H.; Carroll, P. J.; Manor, B. C.; Anna, J. M.; Schelter, E. J. Cerium Photosensitizers: Structure-Function Relationships and Applications in Photocatalytic Aryl Coupling Reactions. *J. Am. Chem. Soc.* **2016**, *138* (18), 5984–5993.
- (10) Ke, X. S.; Ning, Y.; Tang, J.; Hu, J. Y.; Yin, H. Y.; Wang, G. X.; Yang, Z. S.; Jie, J.; Liu, K.; Meng, Z. S.; Zhang, Z.; Su, H.; Shu, C.; Zhang, J. L. Gadolinium(III) Porpholactones as Efficient and Robust Singlet Oxygen Photosensitizers. *Chem. - Eur. J.* **2016**, *22* (28), 9676–9686.
- (11) Yin, H.; Carroll, P. J.; Anna, J. M.; Schelter, E. J. Luminescent Ce(III) Complexes as Stoichiometric and Catalytic Photoreductants for Halogen Atom Abstraction Reactions. *J. Am. Chem. Soc.* **2015**, *137* (29), 9234–9237.
- (12) Abbas, Z.; Dasari, S.; Patra, A. K. Ternary Eu (III) and Tb (III) B-Diketonate Complexes Containing Chalcones: Photophysical Studies and Biological Outlook. *RSC Adv.* **2017**, *7*, 44272–44281.
- (13) Preihs, C.; Arambula, J. F.; Magda, D.; Jeong, H.; Yoo, D.; Cheon, J.; Siddik, Z. H.; Sessler, J. L. Recent Developments in Texaphyrin Chemistry and Drug Discovery. *Inorg. Chem.* **2013**, *52*, 12184–12192.
- (14) Horne, T. K.; Cronjé, M. J. Mechanistic and Photo-Energetics of Macrocycles and Photodynamic Therapy: An Overview of Aspects to Consider for Research. *Chem. Biol. Drug Des.* **2017**, *89*, 221–242.
- (15) Shimanovich, R.; Hannah, S.; Lynch, V.; Gerasimchuk, N.; Mody, T. D.; Magda, D.; Sessler, J.; Groves, J. T. Mn(II)-Texaphyrin as a Catalyst for the Decomposition of Peroxynitrite. *J. Am. Chem. Soc.* **2001**, *123*, 3613–3614.
- (16) Magda, D.; Gerasimchuk, N.; Lecane, P.; Miller, R. A.; Biaglow, J. E.; Sessler, J. L. Motexafin Gadolinium Reacts with Ascorbate to Produce Reactive Oxygen Species. *Chem. Commun.* **2002**, 2730–2731.
- (17) Magda, D.; Miller, R. A. Motexafin Gadolinium: A Novel Redox Active Drug for Cancer Therapy. *Semin. Cancer Biol.* **2006**, *16*, 466–476.
- (18) Magda, D.; Crofts, S.; Lin, A.; Miles, D.; Wright, M.; Sessler, J. L. Synthesis and Kinetic Properties of Ribozyme Analogues Prepared Using Phosphoramidite Derivatives of Dysprosium(III) Texaphyrin. *J. Am. Chem. Soc.* **1997**, *119*, 2293–2294.
- (19) Thiabaud, G.; McCall, R.; He, G.; Arambula, J. F.; Siddik, Z. H.; Sessler, J. L. Activation of Platinum(IV) Prodrugs by Motexafin Gadolinium as a Redox Mediator. *Angew. Chem., Int. Ed.* **2016**, *55*, 12626–12631.
- (20) Thiabaud, G.; Arambula, J. F.; Siddik, Z. H.; Sessler, J. L. Photoinduced Reduction of Pt(IV) within an Anti-Proliferative Pt(IV)-Texaphyrin Conjugate. *Chem. - Eur. J.* **2014**, *20*, 8942–8947.
- (21) Sessler, J. L.; Mody, T. D.; Hemmi, G. W.; Lynch, V. Synthesis and Structural Characterization of Lanthanide (III) Texaphyrins. *Inorg. Chem.* **1993**, *32*, 3175–3187.
- (22) Ringman, J. M.; Frautschy, S. A.; Teng, E.; Begum, A. N.; Bardens, J.; Beigi, M.; Gyls, K. H.; Badmaev, V.; Heath, D. D.; Apostolova, L. G.; Porter, V.; Vanek, Z.; Marshall, G. A.; Hellemann, G.; Sugar, C.; Masterman, D. L.; Montine, T. J.; Cummings, J. L.; Cole, G. M. Oral Curcumin for Alzheimer's Disease: Tolerability and Efficacy in a 24-Week Randomized, Double Blind, Placebo-Controlled Study. *Alzheimer's Res. Ther.* **2012**, *4*, 43–51.
- (23) Shen, L.; Ji, H. F. The Pharmacology of Curcumin: Is It the Degradation Products? *Trends Mol. Med.* **2012**, *18* (3), 138–144.
- (24) Anand, P.; Sundaram, C.; Jhurani, S.; Kunnumakkara, A. B.; Aggarwal, B. B. Curcumin and Cancer: An "old-Age" disease with an "age-Old" solution. *Cancer Lett.* **2008**, *267* (1), 133–164.
- (25) Valentini, A.; Conforti, F.; Crispini, A.; De Martino, A.; Condello, R.; Stellitano, C.; Rotilio, G.; Ghedini, M.; Federici, G.; Bernardini, S.; Pucci, D. Synthesis, Oxidant Properties, and Antitumor Effects of a Heteroleptic palladium(II) Complex of Curcumin on Human Prostate Cancer Cells. *J. Med. Chem.* **2009**, *52* (2), 484–491.
- (26) Siviero, A.; Gallo, E.; Maggini, V.; Gori, L.; Mugelli, A.; Firenzuoli, F.; Vannacci, A. Curcumin, a Golden Spice with a Low Bioavailability. *J. Herb. Med.* **2015**, *5* (2), 57–70.
- (27) Baell, J. B. Feeling Nature's PAINS: Natural Products, Natural Product Drugs, and Pan Assay Interference Compounds (PAINS). *J. Nat. Prod.* **2016**, *79*, 616–628.
- (28) Heger, M.; van Golen, R. F.; Broekgaarden, M.; Michel, M. C. The Molecular Basis for the Pharmacokinetics and Pharmacodynamics of Curcumin and Its Metabolites in Relation to Cancer. *Pharmacol. Rev.* **2014**, *66* (1), 222–307.
- (29) Nelson, K. M.; Dahlin, J. L.; Bisson, J.; Graham, J.; Pauli, G. F.; Walters, M. A. The Essential Medicinal Chemistry of Curcumin. *J. Med. Chem.* **2017**, *60* (5), 1620–1637.
- (30) Gordon, O. N.; Luis, P. B.; Sintim, H. O.; Schneider, C. Unraveling Curcumin Degradation: Autooxidation Proceeds through Spiroepoxide and Vinyl ether Intermediates En Route to the Main Bicyclopentadione. *J. Biol. Chem.* **2015**, *290* (8), 4817–4828.
- (31) Banerjee, S.; Chakravarty, A. R. Metal Complexes of Curcumin for Cellular Imaging, Targeting, and Photoinduced Anticancer Activity. *Acc. Chem. Res.* **2015**, *48* (7), 2075–2083.
- (32) Kljun, J.; Turel, I. -Diketones as Scaffolds for Anticancer Drug Design – From Organic Building Blocks to Natural Products and Metallo-drug. *Eur. J. Inorg. Chem.* **2017**, *33*, 1655–1666.
- (33) The two polyethylene glycol chains and the two propyl alcohols present on the texaphyrin ring confer adequate water solubility to the parent complexes MGd and MLu. The slight increase in the solubility of curcumin is attributed to the interaction with MGd and MLu.
- (34) Hussain, A.; Somyajit, K.; Banik, B.; Banerjee, S.; Nagaraju, G.; Chakravarty, A. R. Enhancing the Photocytotoxic Potential of Curcumin on Terpyridyl lanthanide(III) Complex Formation. *Dalt. Trans.* **2013**, *42*, 182–195.
- (35) Gordon, O. N.; Schneider, C. Vanillin and Ferulic Acid: Not the Major Degradation Products of Curcumin. *Trends Mol. Med.* **2012**, *18* (7), 361–363.
- (36) Katsuyama, Y.; Kita, T.; Funa, N.; Horinouchi, S. Curcuminoid Biosynthesis by Two Type III Polyketide Synthases in the Herb *Curcuma Longa*. *J. Biol. Chem.* **2009**, *284* (17), 11160–11170.